J|A|C|S COMMUNICATIONS

Published on Web 12/23/2009

Combining Aurophilic Interactions and Halogen Bonding To Control the Luminescence from Bimetallic Gold−Silver Clusters

Antonio Laguna,[†] Tania Lasanta,[‡] José M. López-de-Luzuriaga,*[,‡] Miguel Monge,[‡] Panče Naumov,[§] and M. Elena Olmos[‡]

Departamento de Química Inorgánica, Instituto de Ciencia de Materiales de Aragón, Universidad de Zaragoza-CSIC, 50009 Zaragoza, Spain, Departamento de Química, Universidad de la Rioja, Grupo de Síntesis Química de La Rioja UA-CSIC Complejo Científico Tecnológico, 26001 Logroño, Spain, and Department of Material and Life Science, Graduate School of Engineering, Osaka University, 2-1 Yamada-oka, 565-0871 Suita, Osaka, Japan

Received October 30, 2009; E-mail: josemaria.lopez@unirioja.es

Since the introduction of the term *aurophilicity* by Schmidbaur in 1988[1] to explain the short distances between gold(I) atoms observed in the solid state, the increasing amount of experimental evidence of the existence of the aurophilic interaction (AI) in gold complexes has invoked numerous studies that have provided the basis for a description of important relativistic effects. The concept was later expanded to include interactions between other metals in which the metal atoms are separated by less than the van der Waals limit; typically, these include the combination of gold(I) with other closed-shell metals or between metals with either identical (d^{10}−d^{10}) or different (e.g., s^2−d^8, d^8−d^{10}) configurations.[2] In fact, the theoretical treatments have regarded the AI as a more general phenomenon that includes a significant contribution from dispersion forces reinforced by relativistic effects, pointing out the gold-containing structures as a special case where both of these two components are at their maximum.[3] In addition to the fundamental relevance of the AI, the related heterometallic complexes are of interest because of their unconventional photophysical properties, most notably their very efficient luminescence.[4] The *halogen bond* (XB),[5] on the other hand, has attracted much attention recently as a relatively unexploited intermolecular interaction. It appears as a notably strong (5−180 kJ·mol^{-1}) and directional interaction D···X−Y (Y = C, N, halogen, etc.) between a halogen atom (X) and a Lewis base as an electron donor (D). The XB is of critical relevance to the structure and properties of halogen-containing systems and has already been successfully applied in the fields of crystal engineering, superconductors, liquid crystals, and analytical separation as well as to explain substrate−receptor interactions.[5] To provide a qualitative assessment of the relative importance of AIs and XBs in determining the luminescence from gold-containing metal clusters, here we combined these interactions in a series of novel bimetallic Au−Ag structures. We utilized the 4-C_6F_4I group as a ligand because of the strong affinity and lack of steric hindrance of the *p*-iodine for halogen bonding. Some of the new materials exhibit remarkable mechanochromic and luminescent properties; moreover, they are vapochromic, and the luminescence color can be switched rapidly by short exposure to solvent vapors.

The reaction of $Bu_4N[Au(4\text{-}C_6F_4I)]$ (**1**) with $AgClO_4$ afforded the precursor $[Au_2Ag_2(4\text{-}C_6F_4I)_4]_n$ (**2**) as creme-colored solid [details of the syntheses are described in the Supporting Information (SI)]. When as-obtained **2** is exposed to air, it starts to emit bright-yellow light (Figure S1 in the SI). The emission color of **2** can also be switched by shear-induced stress: partial amorphization by grinding [as indicated by powder X-ray diffraction (XRD)] results in a remarkable change of the luminescence color to bright-orange (Figure 1a−d). Fackler and co-workers[6a] and Lee and Eisenberg[6b] have reported on similar grinding-stimulated luminescence phenomena. The behavior observed

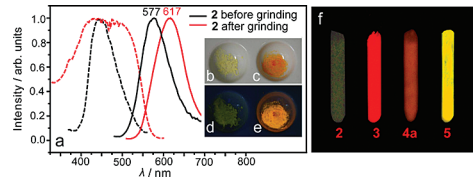

Figure 1. (a) Solid-state spectra and (b−e) mechanochromism of **2** (b, d) before and (c, e) after grinding (dashed line, absorption; solid line, emission). (f) Luminescence of excited **2** (before grinding), **3**, **4a**, and **5**.

Scheme 1. (left) Vapochromic Reactions of **2**−**5** and (right) Dimer−Polymer Equilibrium of the $[Au_2Ag_2(4\text{-}C_6F_4I)_4]$ Cluster

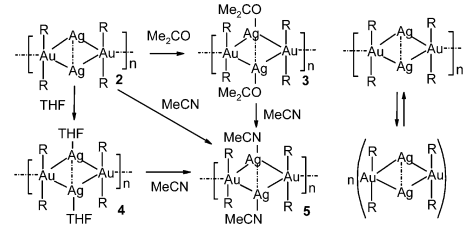

here seems to be different from that described by Lee and Eisenberg,[6b] where the luminescence tribochromism was related to a chemical reaction. Notably, solid **2** is selectively vapochromic toward coordinating solvents: whereas Et_2O and toluene do not react, brief exposure to Me_2CO, THF, or MeCN vapors results in a rapid color change. The products, which were obtained as pure phases by recrystallization from the respective solvents and characterized by X-ray diffraction (Figures S2−S5) are bright-colored: the solvates with Me_2CO (**3**), THF (**4**), and MeCN (**5**) are dark-red, red, and orange, respectively, and they emit vivid red, dark-red and bright-yellow light (Figure 1e and Table 1). From THF, two structural isomers were obtained: **4a** (the thermodynamic isomer) and **4b** (the kinetic isomer). The compositions of the solvates were established as $[Au_2Ag_2(4\text{-}C_6F_4I)_4L_2]_n \cdot xL$, where L = Me_2CO (x = 2; **3**), THF (x = 0; **4**), and MeCN (x = 0; **5**). Similar to **2**, compounds **3** and **4** are vapochromic; the luminescence color can be switched rapidly by exposure to solvent vapors according to the reactions shown in Scheme 1. In situ single-crystal XRD showed loss of crystallinity, evidencing large structure perturbations. The XRD analyses of **3**−**5** revealed that all of the structures are based upon the $Au_2Ag_2(4\text{-}C_6F_4I)_4$ cluster. However, whereas in **3**, **4a**, and **5** the clusters are connected into infinite polymeric chains by Au−Au interactions, in the kinetic isomer **4b**, they exist as monomers that are connected to each other by I···Au interactions (Figure 2).

What are the major structural factors driving the drastic vapochromic switching of luminescence? The stability order of single crystals in air (XRD) is **5** ≫ **4** > **3**.[7] Thus, the reactivity pathways shown in Scheme 1 are determined by the relative coordination ability of the solvent. Moreover, the spectral and structural results

[†] Universidad de Zaragoza.
[‡] Universidad de La Rioja.
[§] Osaka University.

10.1021/ja909241m

Table 1. Selected Structural (Å) and Spectral (nm) Data for **2**−**5**

	d(Au···Au)	*d*(Au···Ag)	*d*(Ag···Ag)	*d*(I···A)	λ_{em}(RT)	λ_{em}(77 K)
2	–	–	–	–	577	600
3	2.7853(14)	2.6814(16) 2.7105(16)	2.966(3)	2.837(23) (A = O)	603	680
4a	2.8738(9)−2.8989(12)	2.6607(15)−2.8314(15)	2.8123(18)−2.889(2)	3.338(10)−3.494(15) (A = F)	611	643
4b	–	2.6922(4) 2.7893(4)	2.8799(7)	3.3420(5) 3.4474(5) (A = Au)	577	614
5	2.9481(3)	2.7377(4) 2.7580(5)	3.1386(9)	3.208(1) (A = N)	575	584, 648(sh)

in Table 1 suggest that two factors drive the vapochromic switching of the luminescence color: (a) the degree of cluster aggregation (polymeric complexes vs **4b**; Figure S6) and (b) the geometry of the Au_2Ag_2 cluster (**1**−**3**, **4a**, and **5**). The latter is affected by the nature of the solvent ligand, and in the absence of other strong intermolecular interactions, it is dominated by the XBs. The aggregation-specific effects (Scheme 1) were assessed from the effect of concentration on the excitation and emission spectra of **3** and **4** in the respective solvents (Me_2CO and THF; Figure 3 and Figure S7). The formation of oligomers, which occurs at high concentrations, results in decreased emission from the $\pi-\pi^*$ transition of the $[Au(4\text{-}C_6F_4I)_2]^-$ unit at 445 nm and concomitant evolution and red shift of another band at 520−575 nm for **3** and 502−570 nm for **4**. Both the excitation and emission spectra are devoid of isosbestic points, and the maxima exhibit a linear dependence on the inverse concentration (Figures S6 and S7). The extrapolated values of λ_{max}^{ex} and λ_{max}^{em} in the solution of **3** (441 and 588 nm, respectively) compare well with the respective experimental solid-state maxima (448 and 603 nm). As expected from the gradual polymerization in solution, for **4**, the extrapolated λ_{max}^{ex} at 450 nm and λ_{max}^{em} at 627 nm reproduce the values of the polymeric structure **4a** (λ_{max}^{ex} = 503 nm, λ_{max}^{em} = 611 nm) better than those of the monomeric isomer **4b** (λ_{max}^{ex} = 522 nm, λ_{max}^{em} = 577 nm). Thus, the stepwise self-assembly of the Au_2Ag_2 clusters into thermodynamically stabilized oligomers lowers the emission energy and causes a red shift in the luminescence wavelength.

To assess the effects of the cluster geometry and, indirectly, the intermolecular interactions, the molecular orbitals (Figure S16) and DFT/TD-DFT excitation spectra (Figures S8−S12) were calculated on the basis of the experimental geometries of the $[Au_2Ag_2(4\text{-}C_6F_4I)_4(Me_2CO)_2]_2$ and $[Au_2Ag_2(4\text{-}C_6F_4I)_4(THF)_2]_2$ units as models for the C_2 tetranuclear clusters in polymeric **3** and the C_i clusters in monomeric **4b**, respectively. In the case of **3**, the highest occupied orbitals, including the relevant HOMO-1, are mainly spread over the 4-C_6F_4I ligands, but there is also a contribution with $5d_{z^2}\sigma^*$ character from the Au(I) centers, as expected for the Au−Au interaction. The LUMO displays 5pσ bonding density between the Au(I) atoms as well as bonding density between the interacting silver centers. In the case of **4b**, the lowest-lying orbitals, including the HOMO, are also centered on the 4-C_6F_4I ligands, with only minor contributions from the metals, but the LUMO is spread over the interacting Ag(I) and Au(I) centers. This implies that the emission wavelength is mainly determined by aggregation through energy modulation of the LUMOs. The intermolecular effects, such as the XBs, affect the emission energy through the HOMOs, which are located at the 4-C_6F_4I ligands. Notably, instead of a HOMO−LUMO transition between Au(I)-centered orbitals, as would be expected for C_6H_5 ligands,[8] the four lowest transitions in the case of the 4-C_6F_4I ligand occur from orbitals on the $[Au(4\text{-}C_6F_4I)_2]^-$ units to a single LUMO centered on the Au_2Ag_2 core. Apparently, the perhalogenation plays a critical role in the communication of the effects of the intermolecular interactions to the emission. Accordingly, whereas the 4-C_6F_4I ligands in **4a**, **4b** and **5** utilize their iodine atom for I···F, I···Au or I···N contacts, one of the ligands in **3** is an I···O halogen bonded [2.837(23) Å] to a noncoordinated acetone molecule. Notably, the Au−Au distance [2.7853(14) Å] and the Au−Ag distance [2.6814(16) Å] for **3** are the shortest within the $[Au_2M_2(C_6F_5)_4L_2]_n$ complexes [Au−Au, 2.8807(4)−3.1959(3) Å; Au−Ag, 2.7267(5)−2.7903(9) Å]. The cluster compression in **3** causes a strong red shift in the emission energy to the red region at 603 nm. The same compound also exhibits the largest red shift (1877 cm^{-1}) on cooling. On the basis of these observations, we envisage utilization of XBs and AIs for control of the (vapo)luminescent properties in similar systems in the future.

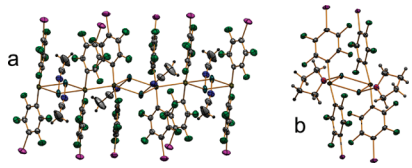

Figure 2. Structures of (a) polymeric **5** and (b) monomeric **4b** motifs.

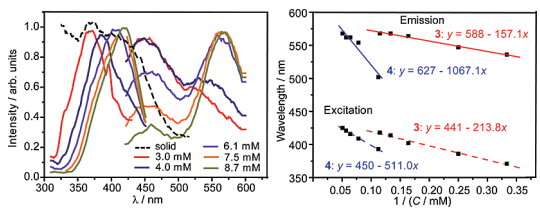

Figure 3. (left) Excitation and emission profiles of solid **3** and **3** in Me_2CO at different concentrations. (right) Linear fits of the excitation and emission maxima of **3** (red) and **4** (blue) vs 1/*C* in Me_2CO and THF, respectively.

Acknowledgment. This work was supported by Project D.G-.I.(MEC)/FEDER (CTQ2007-67273-C02-02). T.L. thanks the M.I-.C.INN for a grant. This work is dedicated to Prof. John P. Fackler, Jr., on the occasion of his 75th birthday.

Supporting Information Available: Experimental and theoretical details, plots of crystal structures (CIF), relevant orbitals, and spectra. This material is available free of charge via the Internet at http://pubs.acs.org.

References

(1) Schmidbaur, H. *Chem. Soc. Rev.* **2008**, *37*, 1931.
(2) Pyykkö, P. *Chem. Rev.* **1997**, *97*, 597.
(3) Fernández, E. J.; López-de-Luzuriaga, J. M.; Monge, M.; Rodríguez, M. A.; Crespo, O.; Gimeno, M. C.; Laguna, A.; Jones, P. G. *Chem.—Eur. J.* **2000**, *6*, 636.
(4) López-de-Luzuriaga, J. M. In *Modern Supramolecular Gold Chemistry: Gold−Metal Interactions and Applications*; Laguna, A., Ed.; Wiley-VCH: Weinheim, Germany, 2008; p 347.
(5) (a) Metrangolo, P.; Neukirch, H.; Pilati, T.; Resnati, G. *Acc. Chem. Res.* **2005**, *38*, 386. (b) Metrangolo, P.; Carcenac, Y.; Lahtinen, M.; Pilati, T.; Rissanen, K.; Vij, A.; Resnati, G. *Science* **2009**, *323*, 1461.
(6) (a) Assefa, Z.; Omary, M. A.; McBurnett, B. G.; Mohamed, A. A.; Patterson, H. H.; Staples, R. J.; Fackler, J. P., Jr. *Inorg. Chem.* **2002**, *41*, 6274. (b) Lee, Y.-A.; Eisenberg, R. *J. Am. Chem. Soc.* **2003**, *125*, 7778.
(7) Compound **2** could be obtained only as a powder.
(8) Fernández, E. J.; Gimeno, M. C.; Laguna, A.; López-de-Luzuriaga, J. M.; Monge, M.; Pyykkö, P.; Sundholm, D. *J. Am. Chem. Soc.* **2000**, *122*, 7287. (b) Fernández, E. J.; Laguna, A.; López-de-Luzuriaga, J. M.; Monge, M.; Montiel, M.; Olmos, M. E.; Rodríguez-Castillo, M. *Organometallics* **2006**, *25*, 3639.

JA909241M